Russian Chemical Reviews **76** (8) 699 – 713 (2007) © 2007 Russian Academy of Sciences and Turpion Ltd

DOI 10.1070/RC2007v076n08ABEH003722

Pulsed EPR in the method of spin labels and probes

S A Dzuba

Contents

I.	Introduction	699
II.	EPR spectroscopy of nitroxide radicals — the fundamentals	699
III.	Pulsed EPR techniques	702
IV.	Structural studies of spin-labelled systems	706
V.	Studies of the dynamics of spin-labelled systems	709
VI.	Conclusion	711

Abstract. Various pulsed EPR in the method of spin labels and probes based on electron spin echo spectroscopy (spin echo envelope modulation through electron – nuclear interactions, electron – electron double resonance, echo detected EPR, *etc.*) are considered. These methods provide information on the conformations of complex biomolecules, nanostructure of matter, depth of water penetration into biological membranes, supramolecular structure of multicomponent systems (membrane – peptide, *etc.*), co-operative orientational dynamics of molecules and dynamic low-temperature transitions in disordered molecular media and biosystems. The bibliography includes 130 references.

I. Introduction

The method of spin labels and probes has been widely used in physicochemical and biophysical studies since the 1970s.[1–3] Spin probes are stable paramagnetic molecules (usually, nitroxyl radicals[4,5]) that are introduced into the system under study as a minor additive. Spin labels represent nitroxide radicals covalently bound to macromolecules. The method of spin labels and probes is used in studies of the local structure of molecules and molecular dynamics, for identification of particular functional groups, measurement of oxygen concentration and proton content, determination of polarity, acceleration of nuclear spin relaxation in MRI studies and for solving some other problems.†

The method makes use of unpaired electrons present in radicals, which permits utilisation of electron paramagnetic resonance (EPR) spectroscopy. Despite the fact that EPR spectroscopy emerged more than six decades ago, the state-of-the-art in this field is characterised by continuous progress and improvement of various experimental techniques. Quite recently, pulsed EPR spin label – spin probe studies began using, in particular, pulsed electron – electron double resonance (PELDOR), electron spin echo envelope modulation (ESEEM), pulsed electron – nuclear resonance, echo-detected EPR, *etc*. All of them are based on the ESE technique.[6,7]

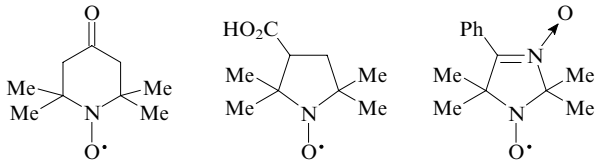
Pulsed EPR spectroscopy significantly extended the potential of the method of spin labels and probes. It allows one to investigate the nanostructure of matter including large biomolecules, supramolecular structure of complex systems, *e.g.*, membranes and their peptide components as well as co-operative small-amplitude orientational motions of molecules in disordered media and biological liquids.

There are a number of reviews[8–15] concerning particular aspects of pulsed EPR spin label – spin probe studies. The main goal of this review was to briefly outline the fields of application of the method, to summarise the results of recent investigations and to highlight new experimental techniques.

II. EPR spectroscopy of nitroxide radicals — the fundamentals

1. Nitroxide radicals. Site-directed spin labelling technique

Nitroxide radicals are stable paramagnetic molecules containing a paramagnetic NO fragment bearing an unpaired electron.[4,5] This fragment is surrounded by the shielding substituents (usually, methyl groups). To date, a few hundreds of nitroxide radicals have been synthesised. A few simple examples are given below:



The so-called site-directed spin labelling (SDSL) technique appeared to be of particular importance for obtaining information on the molecular level.[16–18] The method involves attachment of a spin label to the molecular fragment of interest in a complex biomolecule or supramolecular system. In protein studies, a cysteine residue in the amino acid sequence is most often labelled using a methanethiosulfonate spin label, namely,

S A Dzuba Institute of Chemical Kinetics and Combustion, Siberian Branch of the Russian Academy of Sciences, ul. Institutskaya 3, 630090 Novosibirsk, Russian Federation. Fax (7-383) 330 73 50, tel. (7-383) 330 91 50, e-mail: dzuba@kinetics.nsc.ru

Received 17 April 2007
Uspekhi Khimii **76** (8) 752 – 767 (2007); translated by A M Raevskiy

† According to the IUPAC Compendium of Chemical Terminology (2nd Edition, 1997), the use of the prevailing terms 'nitroxyl radicals' and 'nitroxides' as a class name for 'aminoxyl radicals' is not desirable.

(1-oxyl-2,2,5,5-tetramethylpyrrolin-3-yl)methyl methanethiosulfonate (MTSL). Artificial protein analogues containing this residue are also studied. It is possible to label some other amino acid residues, *e.g.*, lysine, aminoisobutyric acid, *etc*. Small spin-labelled peptides containing less than 50 amino acids and bearing spin labels at desired positions of the amino acid sequence can directly be synthesised. Not only peptides and proteins, but also other biomolecules (*e.g.*, lipids) can be site-directed spin labelled.

2. EPR spectra of nitroxide radicals. Electron – nuclear interactions. The effects of motion

In the framework of the first-order perturbation theory, the X-band (wavelength about 3 cm, frequency ~ 10 GHz) EPR condition for nitroxide radicals can be quite correctly approximated by [19]

$$g(\theta,\varphi)\beta B + a(\theta,\varphi)M = \hbar\omega, \tag{1}$$

where

$$g(\theta,\varphi) = g_{XX}\sin^2\theta\cos^2\varphi + g_{YY}\sin^2\theta\sin^2\varphi + g_{ZZ}\cos^2\theta,$$

$$a(\theta,\varphi) = \sqrt{A_{XX}^2\sin^2\theta\cos^2\varphi + A_{YY}^2\sin^2\theta\sin^2\varphi + A_{ZZ}^2\cos^2\varphi},$$

β is the Bohr magneton; B is the magnetic field induction; M is the nuclear spin projection on the quantisation axis; $\hbar$ is the Planck constant; ω is the frequency of the alternating magnetic field; g_{XX}, g_{YY} and g_{ZZ} are the principal values of the g-tensor; and A_{XX}, A_{YY} and A_{ZZ} are the principal values of the hyperfine coupling tensor. Usually, the molecular system of coordinates is used, in which the X axis is aligned with the N–O bond and the Z axis is normal to the plane in which the >N–O fragment is situated. The angles θ and φ define the direction of the magnetic field in the spherical system of coordinates. Typical values of the components of the magnetic tensors of nitroxide radicals are as follows: $g_{XX} \approx 2.0090$, $g_{YY} \approx 2.0060$, $g_{ZZ} \approx 2.0025$, $A_{XX}/g_e\beta \approx A_{YY}/g_e\beta \approx 5$ G, $A_{ZZ}/g_e\beta \approx 35$ G (g_e is the g-factor of free electron). In the case of high-field EPR, Eqn (1) should be augmented with a term corresponding to the Zeeman interaction between atomic nuclei.

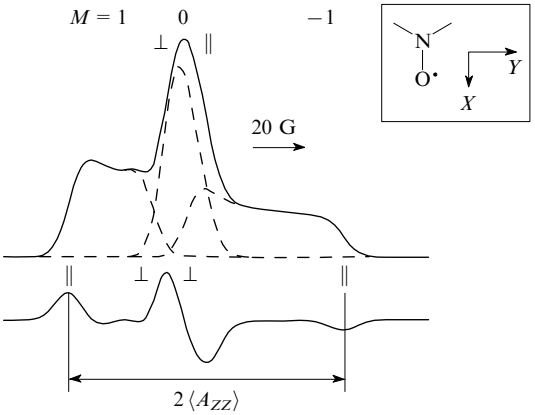


Figure 1. EPR spectrum of a nitroxide radical.
The lower curve represents the EPR spectrum as the first derivative of the absorption lineshape with respect to the magnetic field. Dashed lines denote particular components of HFC; for each component, approximate positions of the parallel and perpendicular orientations are shown. The inset specifies the molecular system of coordinates. The splitting between the outermost peaks in the lower curve approximately equals the doubled A_{ZZ} principal value of the HFC tensor [averaged value is $\langle A_{ZZ}\rangle$ in the presence of librations].

The overall shift of the resonance due to unresolved hyperfine coupling (HFC) of the unpaired electron with other nuclei in the radical and matrix is about 3 G. In the c.w. EPR spectrum, these couplings remain unresolved due to superposition of many lines with small splittings; it should be noted that signals from radicals characterised by different $g(\theta,\varphi)$ values may appear in the same spectral region.

The c.w. EPR technique involves sweep of the field B under continuous action of alternating microwave field at a constant frequency ω. Figure 1 shows a typical shape of the EPR spectrum of a nitroxide radical. Usually, the first derivative of the absorption lineshape with respect to the magnetic field is measured. The parallel and perpendicular orientations of the molecule are also shown; this can be done assuming axial symmetry of the magnetic tensors (see above) and ignoring unresolved hyperfine coupling.

Orientational motions cause averaging of magnetic interactions. In the X-band, the characteristic frequency variation due to different molecular orientations is $\sim 10^9$ rad s^{-1}. Therefore, in the case of fast motions of the whole molecule at frequencies much higher than 10^9 rad s^{-1} the EPR spectrum should exhibit three lines of equal intensity corresponding to three projections of the nitrogen spin on the direction of the external magnetic field. Here, the g-tensor and the HFC tensor are averaged to the scalar values equal to 1/3 of the spurs of the tensors.

Biological and other supramolecular systems are usually characterised by slow molecular motions at frequencies lower than 10^9 rad s^{-1}. As a consequence, no complete averaging occurs; therefore, the results obtained in conventional c.w. EPR experiments are often ambiguous. Pulsed methods based on the ESE technique are sensitive to motion even under glass transition conditions.

3. Electron – electron dipole – dipole interactions between radicals

At present, the dipole–dipole (d–d) interaction between electron spins in spin labels is widely used in studies of the nanostructure of spin-labelled systems. This interaction is of the order of $g_e^2\beta^2/r^3$ in magnitude, where r is the distance between two radicals. Pulsed EPR methods based on the ESE technique are highly sensitive to d–d-interaction. The characteristic times of transverse relaxation in organic solids are about 10^{-6} s and thus the upper bound of the measured distances is nearly 5 to 7 nm. The lower bound obtained from the 'dead time' of an instrument ($\sim 10^{-7}$ s) is close to 1.5 nm. The advantage of ESE spectroscopy consists of high accuracy of measurements in this range of distances. At $r \sim 3$ nm, the error is at most 0.1 nm.[8–10] This is a record spatial resolution among all known physical methods, which allows one to reveal subtle effects in the nanostructure of matter that cannot be disclosed by other methods. It should also be noted that ESE studies do not require special treatment of samples (*e.g.*, crystallisation, high degree of purification, *etc*.)

The Hamiltonian of magnetic dipole–dipole interactions between the magnetic moments of two electrons has the form

$$H_d = g_1 g_2 \beta^2 \frac{r^2 \boldsymbol{S}_1\boldsymbol{S}_2 - (\boldsymbol{S}_1\boldsymbol{r})(\boldsymbol{S}_2\boldsymbol{r})}{r^5}, \tag{2}$$

where g_1 and g_2 are the g-factors of two particles; $\boldsymbol{S}_1$, $\boldsymbol{S}_2$ are the spin operators; $\boldsymbol{r}$ is the radius vector connecting the particles. Almost all long-chain biradicals can be studied in the point dipole approximation, which assumes that the spin density of the unpaired electron is localised at some point.[10]

When studying nitroxide biradicals, one can use the perturbation theory, which treats the Hamiltonian (2) as a small

perturbation compared to expression (1). In the case of weak d–d-interactions, where

$$\varepsilon_d \ll |g_1 - g_2|\beta B$$

(this is always valid at $r > 0.15$ nm), the transition frequencies for each of the two spins are given by [10]

$$\omega_{1,2} = \frac{g_{1,2}\beta}{\hbar} B \pm \frac{1}{2}\varepsilon_d , \quad (3)$$

where

$$\varepsilon_d = \frac{g_1 g_2 \beta^2}{r^3 \hbar}(1 - 3\cos^2 \Theta),$$

(Θ is the angle between the direction of the external magnetic field and the line connecting two radicals). The sign $\pm$ means that for each spin the resonance is shifted due to the d–d-interaction with the partner spin depending on the projection of the latter on the direction of the external magnetic field.

Considering pulsed EPR methods, expression (3) leads to temporal dependences of the type $\cos(\varepsilon_d t)$ (see below).[10] The Fourier-transformed EPR spectrum exhibits a doublet at the frequencies $\pm\varepsilon_d$. In a polyoriented system, the frequency (ω)-dependent intensities of the dipolar doublet lines are averaged over all spatial orientations of the pair. At

$$\omega_\perp = \pm \frac{g_1 g_2 \beta^2}{r^3 \hbar},$$

singularities appear ($\Theta = \pi/2$, perpendicular orientation of the pair). Often, only the singularity due to the relatively low intensity of other lines can be observed experimentally. Its position permits immediate determination of the distance r.

4. Electron spin echo of nitroxide radicals

Excitation of transitions between spin energy levels by intensive microwave pulses causes the appearance of a free induction signal, *i.e.*, an oscillating macroscopic transverse magnetisation.[6,7] Optimum conditions for observation of the free induction signal are attained by applying a pulse that causes a $\pi/2$ (90°) flip of the magnetisation vector. Typical microwave pulse durations in ESE spectrometers are 10 to 100 ns. Signal decay is due to the scatter of precession frequencies (this determines the shape of the EPR spectrum).

The resolution of ESE spectrometers is limited by the characteristic time of transient processes in the cavity upon application of microwave pulses (usually, it is of the order of 100 ns),[6,7] which is called the 'dead' time. In the case of nitroxide radicals, the nonzero 'dead' time makes observation of the free induction signal impossible owing to fast signal decay. The free induction signal can only be observed after some hardware improvements aimed at shortening the 'dead time', *e.g.*, on going to the Ku-band (resonance frequency 17 GHz, not to be confused with the Q-band!) and to elevated temperatures (this is required for line narrowing).

Two pulses applied with a time delay cause the appearance of an echo signal (see Fig. 2 *a*). The time delay after the second pulse equals the time delay between two pulses, τ. The optimum flip angle of the magnetisation vector upon application of the second pulse is π. The formal notation for the pulse sequence and the echo signal is given below:

$$\pi/2 - \tau - \pi - \tau - \text{echo}.$$

The mechanism of the appearance of the echo signal is as follows. The second pulse follows the first one after the time delay τ and changes the phase of spin precession in the plane normal to the external magnetic field. Now the precessing spins

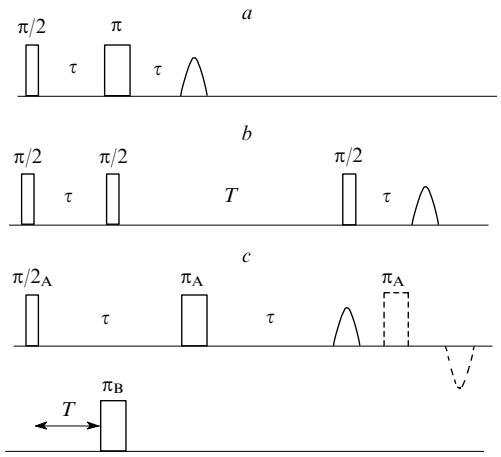


Figure 2. Electron spin echo pulse sequences.
Basic two-pulse sequence (*a*), three-pulse stimulated echo sequence (*b*) and two-frequency double resonance (PELDOR) (*c*). PELDOR experimental conditions: detection at the A spin frequency and an additional pump pulse at the B spin frequency. Dashed lines show an additional refocussing pulse and echo (see text).

have the same velocities but different initial phases. At the instant τ after the second pulse, refocussing occurs (all spins have the same phase) and the echo signal appears (then, defocussing will occur again). The echo signal decays with increase in τ due to spin relaxation.

Yet another method for ESE detection is the three-pulse stimulated echo pulse sequence (Fig. 2 *b*)

$$\pi/2 - \tau - \pi/2 - T - \pi/2 - \tau - \text{echo}.$$

The first pulse creates a precessing transverse magnetisation and the second pulse creates the projection of the magnetisation vector on the Z axis (longitudinal magnetisation), which retains its magnitude during the time T in the absence of relaxation. This pulse creates a nuclear coherence, *i.e.*, the system is described by a non-stationary superposition of various electron–nuclear states upon application of the second pulse. The third pulse again creates the transverse magnetisation, which refocusses at the instant

$$t = 2\tau + T,$$

i.e., the echo signal appears.

A feature of the ESE studies of nitroxide radicals consists in incomplete (or selective) excitation of the EPR spectrum by microwave pulses. In most experiments, the pulse amplitudes reach 3–5 G, whereas the overall width of the EPR spectrum is of the order of 70–80 G. In some cases (*e.g.*, in studies of spectral diffusion, *i.e.*, stochastic fluctuations of the resonance frequency due to orientational motion), this feature is of crucial importance.

If orientational motions cause fluctuations of the resonance frequencies with the root-mean-square $\langle\Delta\omega^2\rangle$ and the correlation time τ_c, theory predicts that at

$$\langle\Delta\omega^2\rangle\tau_c^2 \ll 1,$$

the relaxation rate is given by $\langle\Delta\omega^2\rangle\tau_c$.[20] The $\Delta\omega$ value can be estimated with ease from Eqn (1). For simplicity, suppose an axial symmetry

$$g_{XX} = g_{YY} = g_\perp , \; A_{XX} = A_{YY} = A_\perp .$$

Let us denote

$$gzz = g_{\|},\ Azz = A_{\|}\ .$$

In the case of small-amplitude motions the angle θ fluctuates by $\Delta\theta$. Then, in a constant magnetic field B, expansion of the resonance frequency fluctuations $\Delta\omega$ in terms of $\Delta\theta$ has the form [21]

$$\Delta\omega = 2\sin\theta\cos\theta \times \tag{4}$$

$$\times \left[(g_{\perp} - g_{\|})\frac{\beta B}{\hbar} + M\frac{A_{\perp}^2 - A_{\|}^2}{2\hbar\sqrt{A_{\perp}^2\sin^2\theta + A_{\|}^2\cos^2\theta}} \right]\Delta\theta\ .$$

At $\theta = 0$, π and $\pi/2$, the $\Delta\omega$ value equals zero, *i.e.*, spin relaxation near the canonical orientations (parallel and perpendicular) should be slow.

Fast small-amplitude orientational motions also manifest themselves in c.w. EPR spectra, because they cause partial averaging of anisotropic magnetic interactions. In the case of orientational motion about an axis lying in the XY plane of the molecular system of coordinates, the parameter $A_{\|}$ is averaged [22]

$$\langle A_{\|}\rangle = A_{\|} - (A_{\|} - A_{\perp})\langle\alpha^2\rangle, \tag{5}$$

where the angular deviation, α, from the equilibrium position is related to $\Delta\theta$ as follows: $\Delta\theta = \alpha\sin\varphi$. The parameter $\langle A_{\|}\rangle$ can be measured with ease from the splitting between the outermost peaks in the EPR spectrum (see Fig. 1).

III. Pulsed EPR techniques

1. ESEEM through electron – nuclear interactions

If an electron spin interacts with a nuclear spin, application of microwave pulses at the EPR resonance frequency causes simultaneous excitation of both allowed and forbidden spin transitions (without and with nuclear spin flip, respectively) in a solid.[6,7] Interference of the resonance frequencies of these transitions upon ESE decay induces beats (oscillations) of the signal, which are called electron – nuclear modulation or the electron spin echo envelope modulation (ESEEM) effect.[6,7] A few examples of the ESEEM effect are shown in Fig. 3 *a*, which corresponds to the interaction between the unpaired electron of the spin label and deuterons from the surrounding heavy water. The Fourier-transformed frequency spectrum of the beats exhibits peaks (see Fig. 3 *b*), the positions of which are determined by the electron – nuclear interactions. In the case of interactions with the nearest nuclei in the matrix, these peaks are centred around the resonance (Larmor) frequency of a given nucleus in the magnetic field of the ESE spectrometer (2.2 MHz for deuterons). These peaks cannot be resolved in c.w. EPR experiments (see above).

The ESEEM through electron – nuclear interactions represents a convenient tool of structural studies in the nearest environment of spin labels; it can be used for identification of the types of the nuclei in the nearest environment and determination of their spatial arrangement relative to the unpaired electron.

This approach has long been used in pulsed EPR spectroscopy, where it can be considered classical. Most related methodological problems have been solved to date. The fundamentals of the ESEEM technique have been comprehensively treated in monographs.[6,7] Recently, this method has found increasing application in studies of the local environment of spin labels.

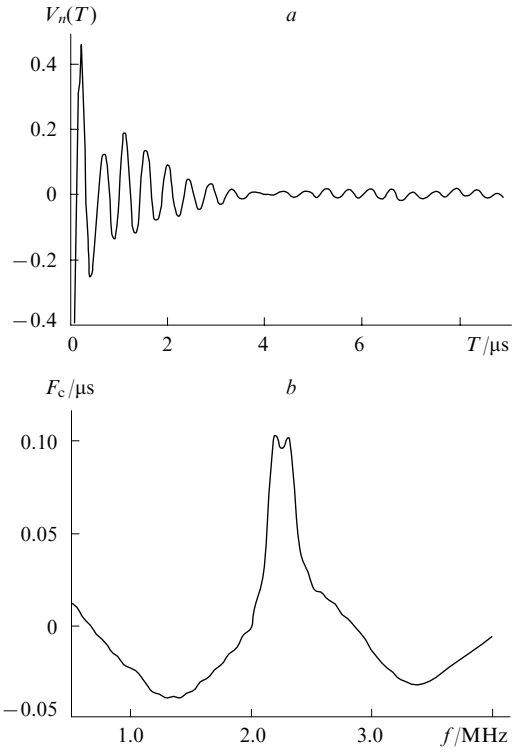


Figure 3. Typical signal oscillations (ESEEM) induced by electron – nuclear interactions (*a*) and Fourier-transformed frequency spectrum (*b*) of a spin label in D_2O-containing matrix.
Rom original experimental ESEEM a smooth non-oscillating function (result of averaging) was subtracted; the resulting $V_n(T)$ signal is normalised to this function at $T = 0$. F_c denotes the Fourier transform amplitude.

2. Pulsed electron – electron double resonance in studies of d – d-interactions between radicals

As mentioned above, the d – d-interaction between radicals is now widely used in studies of the nanostructure of spin-labelled systems. Most of them are carried out by pulsed double electron – electron resonance (PELDOR).[8–10,13] The method was proposed in the 1980s.[23,24] It allows one to determine the distances between radicals on the nanometre scale, draw conclusions on the conformations of doubly spin-labelled biomolecules and estimate the size of the aggregate (cluster) of spin-labelled molecules in the case of their aggregation (clusterisation).

In the PELDOR experiments the echo signal appears upon application of a conventional two-pulse sequence and an additional 180° pump pulse at the other resonance frequency (Fig. 2 *c*). The spins responsible for the appearance of the echo signal are called A spins while their partner spins (in our case, they are influenced by the additional pulse) are called B spins. The phase of the A spins at $t = 2\tau$ equals

$$\varphi_A = \pi \pm \varepsilon_d T$$

(the 'plus' or 'minus' sign depends on the projection of the B spin).

The echo signal is proportional to $\cos(\varepsilon_d T)$, which means that the signal is modulated at the frequency ε_d as the time T changes. Note that here modulation is due to electron – electron rather than electron – nuclear interactions (see above). The Fourier transform of the modulated ESE decay in a polyoriented system leads to the appearance of a peak at the singularity frequency

$$\omega_{\perp} = \pm \frac{g_1 g_2 \beta^2}{r^3 \hbar}.$$

The separation between spin labels can be determined from the position of this peak.

The effect of finite pulse duration (theory assumes infinitely short pulses) can be eliminated using an additional refocussing pulse.[13]

Pulsed ELDOR technique also allows study on clusterisation of spin-labelled molecules. Actually, the pump pulse excites only a fraction, P_B, of the partner spins of a given A spin. If a cluster comprises N particles and the probability of simultaneous excitation of more than one B spin is low (*i.e.*, $P_B N \ll 1$), the ESE signal is given by [8]

$$V(T) = [1 - P_B\langle 1 - \cos(\varepsilon_d T)\rangle]^{N-1}. \quad (6)$$

It follows that at $t \to \infty$ the $V(T)$ value tends to the limiting value equal to $(1-P_B)^{N-1}$. This asymptotic value can experimentally be measured with ease and thus one can estimate the number of particles, N, in the cluster.

The same effect can be attained not only by irradiating B spins at the other resonance frequency, but also by changing the magnetic field in a pulsed (jumpwise) manner. This experimental technique was practically implemented in the X-band [25] and W-band [26] EPR experiments. The A spins are excited using the three-pulse stimulated echo sequence. In the time between the second and third pulses, the magnetic field is changed in a jumpwise manner and a 180° pump pulse is applied. Due to shift of the resonance, this pulse affects only the B spins. The approach assumes the time delay τ between the first and second pulses to be varied. Here, electron–nuclear modulation also appears in addition to modulation through electron–electron interactions. The two mechanisms can be distinguished by separating the overall decay signal into the decay signal observed in the presence and in the absence of pump (no pump pulse). These mechanisms are independent of each other and should therefore contribute multiplicatively to the observed envelope modulation.

The advantage of the field-step PELDOR over the two-frequency PELDOR technique consists the possibility of using a scanning pump [25] owing to an increase in the proportion of spins P_B to be excited, which leads to an increase in the modulation depth. A drawback of the technique is the effect of transverse relaxation on the echo decay observed.

Various methodological aspects of the PELDOR technique have been considered in a number of recent studies. Mention may be made of the problem of correct inclusion of the spin label structure and binding to a biomolecule in modelling the structure of the biomolecule from PELDOR data.[27] Methodological aspects concerned with extraction of information from PELDOR data and optimisation of experimental design have been considered.[28–30] A comparative PELDOR study of biradicals in two (X and S) EPR bands was carried out.[31] Since the electron–nuclear modulation depends on the particular microwave band while the electron–electron modulation is independent of it, the approach can be employed to determine the contribution of the electron–electron modulation. It was reported [32] that the quality of information extracted from the PELDOR frequency spectra can be improved using isotopic substitution, namely, by replacing (i) ^{14}N atom by ^{15}N atom and (ii) hydrogen atom by deuterium atom in one radical of the pair. Here, the 2D version of the four-pulse PELDOR was proposed as the experimental technique. The potential of PELDOR studies of biradicals in the high-frequency EPR band (frequencies higher than 95 GHz) was discussed.[33] Orientational selectivity effects due to high spectral resolution were demonstrated.

3. Miscellaneous methods of investigation of d–d-interactions

Complications in PELDOR experiments (need for an additional source of microwave radiation, a special cavity, *etc.*) gave an impetus to the development of miscellaneous experimental techniques for studying d–d-interactions.

The '2 + 1' method [34] is similar to the PELDOR technique except for the fact that all pulses are applied at the same resonance frequency. The pulse sequence is as follows:

$$\text{pulse } 1 - T - \text{pulse } (+1) - (\tau - T) - \text{pulse } 2 - \tau - \text{echo}.$$

The echo signal is created by two pulses (pulse 1 and pulse 2); an additional pulse (it is this pulse that is called +1) is necessary to achieve alternation of the d–d-interaction. Experiments involve variation of the time T at constant τ. A drawback of the '2 + 1' method is that it is not free from electron–nuclear ESEEM. Moreover, the dipole–dipole interaction alternates under the action of not only pulse +1, but also the second pulse. Correct allowance for interference between these two effects is not always possible. As a result, information on the d–d-interaction can be significantly distorted.

Method based on double-quantum coherence. Using an appropriately designed pulse sequence, it is possible to excite a double-quantum coherence in the spin level system of a biradical.[35] A commonly used pulse sequence for this experiment includes four pulses. Three of them ($\pi/2$ pulses) create a stimulated echo signal. An additional π pulse is applied at the midpoint of the time interval between the second and third pulses. The contribution of the double-quantum coherence is selected using the pulse phase cycling from one series to another. Experiments involve variation of the time τ; the signal is modulated at the ε_d frequency.

In order to avoid the loss of signal during the 'dead' time, an additional refocussing (fifth) pulse is applied. One can also use the six-pulse sequence, in which the double-quantum coherence is created by three rather than two pulses.

$$\pi/2 - \tau/2 - \pi - \tau/2 - \pi/2.$$

The advantage of this approach consists of the absence of the interference effects characteristic of the '2 + 1' method. However, in this case the electron–nuclear ESEEM occurs too.[36] The drawbacks of the double-quantum coherence technique also include the large number of phase change cycles (a total of sixty-four cycles), which can introduce an additional error, and high demands to experimental equipment, namely, the amplitudes of microwave pulses should be higher than the pulse amplitudes for commercially available spectrometers. Finally, the phenomenon is characterised by a rather complicated theoretical description and the lack of a clear picture. Nevertheless, a number of double-quantum coherence studies of the d–d-interaction of spin probes are available in the literature. Methodological aspects of application of the method have been considered.[37] ESEEM suppression techniques were also proposed.[38]

A method based on the solid-state NMR pulse sequences [39] is based on the known 'solid echo' and Jeener–Broekaert pulse sequences. The 'solid echo' pulse sequence is as follows:

$$(\pi/2)_x - \tau - (\pi/2)_y - \tau - \text{echo}.$$

Compared to the double-quantum coherence method, here the experimental design is much simpler (smaller number of phase change cycles is required). However, theoretical description remains complicated and no clear representation of the phenomenon is available.

The aforesaid suggests that at present PELDOR is the most convenient method of investigation of d – d-interactions. It provides a clear picture of the phenomenon and essentially simplified theoretical description and is almost free from the ESEEM effects. These advantages were demonstrated in a comparative double-quantum coherence and PELDOR study [36] of a doubly spin-labelled protein with a label-to-label separation of 3.55 nm.

4. Relaxation-induced enhancement of electron – electron ESEEM induced by in d – d-interaction

The drawback of all the methods described above including PELDOR is low portion of excited spins (at most 10% – 15%) due to a large width of the EPR spectra of nitroxide radicals compared to the amplitude of microwave pulses; as a consequence, the ESEEM effect is weak. This drawback becomes particularly pronounced on going to high-field EPR. An approach [40] based on the use of spin – lattice (longitudinal) relaxation in the spin pair makes it possible to overcome these difficulties. The Larmor frequency of the resonance A spin coupled with an off-resonance B spin

$$\omega_A^* = \omega_A + m_B\varepsilon_d\,,$$

where m_B is the B spin projection, can be changed by B spin flips induced by longitudinal relaxation. In this case the probability for an odd number of the B spin flips to occur during the time interval T is $0.5[1-\exp(-T/T_1)]$, where T_1 is the longitudinal relaxation time. With scanning τ, the stimulated ESE is modulated at the dipolar frequency ε_d. The modulation amplitude increases with the 'evolution' period T. Relaxation-induced dipolar modulation enhancement (RIDME) was observed experimentally.[40] The RIDME method is free from the drawbacks associated with the low portion of excited spins, because up to 50% of all off-resonance spins can be involved in dipolar modulation. Therefore, RIDME is a quite promising method of high-field ESE studies, as was shown by, *e.g.*, a 130-GHz (4.4 T) ESE.[41]

5. ESEEM modulation due to spontaneous intramolecular motions and nuclear spin relaxation

Modulation phenomena in conventional ESE methods are due to coherent dynamic effects caused by simultaneous excitation of two and more transitions in the EPR spectrum under the action of microwave pulses. In the case of RIDME, the ESE modulation is due to spontaneous changes in the magnetic parameters of radicals under the action of the pulse sequence. However, spontaneous changes can also be induced by intramolecular motions [42] and nuclear spin relaxation in the nearest environment.[43] Such effects are studied using the three-pulse stimulated echo sequence. It includes scanning the time delay τ between the first and second pulses at the fixed time delay T between the second and third pulses. The ESEEM is due to a spontaneous change in the Larmor precession frequency of electron spin in the course of system evolution between the pulses during the time T, induced by longitudinal nuclear spin relaxation in the nearest environment. The longer the time T the more probable the event. Manifestation of spontaneous processes in the ESEEM have been considered in a review.[44]

6. Pulsed high-field/high-frequency EPR

High-field (high-frequency) EPR is observed in magnetic fields higher than 3 T (frequencies higher than 95 GHz). Continuous-wave high-field/high-frequency EPR has long been used in studies of spin-labelled systems. The main advantage of the technique consists of orientation selectivity due to the g-factor anisotropy, which permits investigation of particular (different) orientations of spin probes and spin labels. Therefore, research on polyoriented systems provides information identical to that obtained in studies of oriented single crystals. Recently, a number of pulsed high-field/high-frequency EPR studies of the molecular structure and dynamics of spin-labelled systems have been reported (see, *e.g.*, Refs 26, 33, 41, 45, 46). High-field/high-frequency EPR spectrometers are commercially available.

7. Echo-detected EPR in studies of orientational dynamics

In echo-detected EPR, the echo signal is recorded as the function of the magnetic field at different times τ (2D experiment).[21] Different resonance fields correspond to different orientations of the radical relative to the external magnetic field direction (see Fig. 1); therefore, the method allows one to obtain information on the orientational dependence of the relaxation rate or relaxation anisotropy. The relaxation anisotropy is related to the mechanism and rate of motion.

For convenience, a number of echo-detected EPR spectra are recorded at different τ normalised to the same magnetic field corresponding to the spectral maximum and then plotted together as shown in Fig. 4. This allows one to exclude the magnetic field independent isotropic relaxation governed by some processes not related to motions and to clarify the character of the relaxation anisotropy. For instance, Fig. 4 shows that relaxation near the spectral edges (they correspond to the parallel orientation of the molecule, see Fig. 1) is slower.

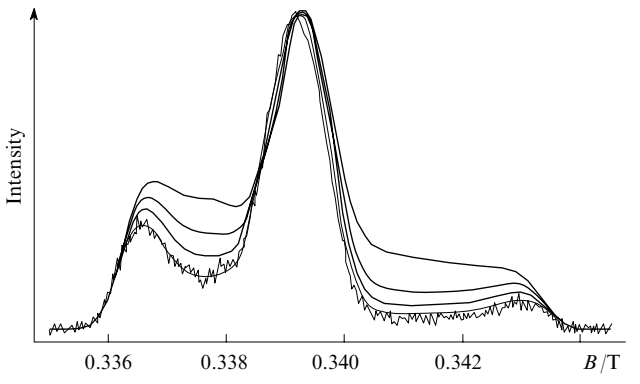


Figure 4. Typical echo-detected spectra recorded at different time intervals τ between pulses and normalised to the maximum intensity.
The thin solid line denotes the results of calculations using the model of fast small-amplitude motions (see text).

Echo-detected EPR of spin probes is sensitive to fast small-amplitude stochastic motions of the spin probe and spin label molecules near equilibrium positions. Such orientational motions are called stochastic librations; they are only characteristic of disordered molecular (including biological) media. The technique is sensitive to very small motion amplitudes (down to 0.1 – 1°).[47] Note that stochastic motions are different from dynamic orientational oscillations that are characteristic of any phase state of matter.

8. Two-dimensional pulsed electron – electron double resonance in studies of orientational dynamics

The pulse sequence of 2D pulsed electron – electron double resonance [12, 48, 49] is the same as the PELDOR pulsed sequence. The difference is that here the free induction signal appeared after application of the last pulse is measured. The Fourier tranform is performed over two times, the time T and the time

delay after the last pulse in the pulse sequence. The 2D spectra allow one to differentiate the homogeneous broadening due to the motion and the inhomogeneous broadening caused by microscopic ordering, *i.e.*, to obtain information on structural dynamic heterogeneity of the system. In this case, observation of the free induction signal requires the use of short-'dead-time' instruments, *e.g.*, Ku-band EPR spectrometers (17 GHz). Line narrowing can be attained at elevated temperatures.

9. Pulsed double electron – nuclear resonance

In addition to ESEEM EPR, electron – nuclear interactions can be studied by c.w. electron – nuclear double resonance (ENDOR) and by pulsed ENDOR according to Mims and Davies. A comparative study [50] of the interaction of spin labels with ^{31}P nuclear spins carried out by different experimental techniques showed that the most reliable data can be obtained using the Mims pulsed ENDOR method, which allows small splittings (to 0.03 MHz; this corresponds to a distance of 1 nm) to be measured. In studies of spin-labelled lipids in a completely hydrated membrane these measurements permit determination of the tilt angles of lipid chains with respect to the membrane plane.

High-field pulsed ENDOR/EPR studies are also possible.[51] Orientation selectivity allows one to obtain more detailed information on the structure of the nearest environment of the molecule under study. This method was used to study the geometry of complexes of spin probes with solvent molecules (*e.g.*, complexes of 5-doxylstearic acid with deuterated alcohols).[51]

10. 'Saturation – recovery' technique in time-resolved EPR

Time-resolved EPR [52] is not a pulsed technique, because the EPR signal is detected using c.w. microwave field. Considering relaxation time measurements, the 'saturation – recovery' technique occupies an intermediate position between the pulsed and c.w. EPR, because it combines pulsed saturation of the EPR spectrum (usually, the saturation pulse is a few microseconds long) and continuous recording of the EPR signal. The method was employed to study acceleration of the spin label relaxation in biosystems induced by the fluctuating magnetic dipole – dipole interaction with the neighbouring metal ion. The results obtained were used for estimating the distance in a pair spin label – ion.[53 – 55]

The 'saturation – recovery' technique is used for the determination of local concentrations of molecular oxygen (so-called oximetry) in biological objects.[56] It is based on acceleration of spin label relaxation by collisions with molecular oxygen.

EPR has an advantage over than the ESE spectroscopy-based techniques, when the ESE (or free induction) signal cannot be observed due to the problems related to the 'dead' time of the spectrometer and short relaxation times. However, the technique is not free from drawbacks including a lower temporal resolution, a complex and ambiguous theoretical description and lower functionality.

There are some interesting applications of time-resolved EPR spectroscopy for solving spin chemistry problems. An example is provided by spin polarisation transfer to the spin label in the molecule of a model hexapeptide from photoexcited chromophore located in the same molecule.[57] Yet another example is the effect of spin labels on the formation of spin polarisation in spin-correlated radical pairs generated upon photoexcitation of photosynthetic reaction centres in plants.[58] The results obtained may be useful in studies of electron transfer in these systems. Pulsed EPR spectroscopy also seems to be useful in this case.

IV. Structural studies of spin-labelled systems

1. Conformations of long-chain biradicals and doubly spin-labelled biomolecules

Different conformations of a molecule have different length. Therefore, the conformational structure of biradicals or doubly spin-labelled biomolecules can be determined by measuring the distances between two unpaired electrons in them. Details of relevant measuring techniques including PELDOR and some other methods have been reviewed (see, *e.g.*, Refs 8 – 10). Now we will discuss the state-of-the-art in the field and recent literature.

Long-chain biradicals can adopt a large number of possible conformations; therefore, one should consider a distance distribution function of paramagnetic fragments. If the distance distribution is expected to be rather narrow, its width can be directly estimated from the ESEEM decay. In particular, a magnetic field jump PELDOR study of two long-chain ($\sim$2 nm long) biradicals (a rigid-chain and a flexible one) was reported.[25] The distance distribution width estimated from the ESEEM decay for the flexible biradical was found to be about 0.3 nm.

Conformations of a biradical containing two nitroxide fragments separated by a chain comprising from 8 to 20 methylene groups (n = 8, ...20) were studied by the PELDOR method.[59,60] A large scatter of distances between the two radicals was expected. The data extracted from the frequency spectra were compared with the results of calculations of (i) fully stretched *trans*-conformation (limiting case) and (ii) conformational statistics at a specified temperature. The results of distance measurements and conformational statistics calculations coincided within the limits of experimental error. At n = 10 and r = 2.1 nm (average distance), the distribution function width at half-height was 0.5 nm.

The PELDOR technique permits measurements of spin – spin interactions not only in nitroxide biradicals, but also in biradicals containing a paramagnetic metal ion as the spin partner.[61]

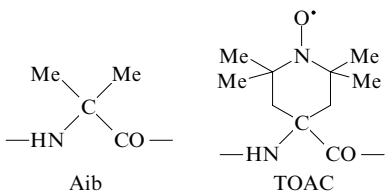
Doubly spin-labelled peptides can also be studied in a similar manner. If the spin labels are separated by a short distance ($<$ 1.5 nm), c.w. EPR spectroscopy is employed.[62] If the label – label distance exceeds 1.5 nm, pulsed EPR techniques should be used.

PELDOR studies of conformations of a doubly spin-labelled peptide Trichogin GA IV in organic glasses are available.[63 – 65] This linear peptide isolated from the fungus *Trichoderma longibrachiatum* is a rich source of aminoisobutyric (Aib) acid

n-Oct-Aib^1-Gly-Leu-Aib^4-Gly-Gly-Leu-Aib^8-Gly-Ile-Lol

(n-Oct is n-octanoyl and Lol is leucinol). Trichogin GA IV possesses antibacterial and antifungal properties. Such peptides can create ionic channels in membranes, thus making them permeable, which may cause cell death. A distinctive feature of Trichogin GA IV is that its molecule is short. It comprises only 10 amino acids, which is much smaller than the membrane thickness; therefore, the mechanism of membrane permeability is unclear as yet.

The Aib residues are replaced by structurally similar nitroxide spin labels (TOAC) in the course of chemical synthesis.[66]



Aib TOAC

For convenience, the peptide terminal groups could be replaced by other residues. This does not change the membrane-modifying properties of the peptides.[67] The peptides synthesised were doubly labelled at positions 1 and 4, 4 and 8 or 1 and 8. The first two types of biradicals can be studied by c.w. EPR spectroscopy, whereas the third type can only be studied by pulsed EPR methods due to long spin–spin separations.

Conformations of doubly spin-labelled peptide were studied at 77 K in different glass-forming solvents (methanol, ethanol, trifluoroethanol) and in chloroform–DMSO mixtures with different component ratios.[63,64] PELDOR studies in all matrices revealed modulation effects at different oscillation frequencies. The distances between the spin labels in positions 1 and 8 vary from 1.53 (in trifluoroethanol) to 2.18 nm (in ethanol). It was concluded that the peptide adopts the 3_{10}-helical conformation in trifluoroethanol and the 2_7-helical conformation in other matrices.

Conformation of spin-labelled Trichogin-1,8 in biological membranes was studied.[68,69] The distance distribution function in egg L-α-phosphatidylcholine membranes exhibits two maxima at 1.3 and 1.8 nm.[68] The authors suggested that the peptide conformations represent combinations of the α-helical conformation, 3_{10}-helical conformation and more stretched conformations. Similar results were obtained for this peptide in model phospholipid membranes.[69]

PELDOR studies of doubly-nitroxide-labelled RNA were reported.[70–72] The label–label distances were found to lie between 2 and 5 nm. The results of measurements were in agreement with the results of molecular dynamics calculations. Based on the results obtained, the conformations of the biomolecules were determined.

Changes in the conformation of a protein (BtuB) upon binding to a substrate (TonB) in a membrane have been a subject of a joint SDSL–PELDOR study.[73] The protein binds and carries vitamin B_{12} across the outer membrane of Gram-negative bacteria such as *Escherichia coli*. The protein was doubly spin labelled. In the absence of the substrate, the results of measurements showed a narrow interspin distance distribution for the number of pairs (number of pairs from r to $r + dr$). In the presence of the substrate, the distance distributions broadened. This indicates a substrate-induced transition of the protein from the ordered to disordered state.

Singly labelled Na^+/H^+ regulators, namely, NhaA from *Escherichia coli* were studied.[74] Residues situated in domains undergoing pH-dependent structural changes were chosen for site-directed spin labelling. PELDOR experiments revealed modulation of the echo signal, which showed that NhaA exists in the dimeric form. The modulation depth reversibly decreased with the decrease in the pH value, thus indicating an increase in the distance in the dimer. Relation between these results and the mechanism of NhaA activity was considered.

The structure of different-size [2]catenanes was studied by the PELDOR method.[75] Each of the two macrocycles was spin labelled. The molecular conformation distribution and size were evaluated by comparing the experimental data and theoretical estimates.

The arrangement of the *b*-subunits in the holo-enzyme F_0F_1-ATP synthase from *E. coli* was investigated by the SDSL and PELDOR methods.[76] Based on the interspin distances, parallel orientation of two helices and other structural features were revealed.

A double-quantum coherence study of model peptide helices was carried out.[77] The intramolecular distances were determined and the folding of the helices was studied.

The possibility of SDSL and PELDOR studies of the global structure of nucleic acids was considered.[78] Spin labelled duplexes of DNA dodecamers with known structure were used as model systems. The distances measured by PELDOR (2 to 4 nm) were in agreement with those obtained from NMR data.

2. Peptide aggregation in molecular glasses and biomembranes

There are reasons to assume that peptide aggregation in biomembranes significantly affects their functional properties, *e.g.*, formation of ionic channels. The sizes of peptide aggregates are on the nanometre scale, which points to the possibility of using the PELDOR method.

To clarify possible mechanisms of peptide aggregation in biomembranes, peptides in simpler model systems were studied. The results of the PELDOR studies of aggregation of spin-labelled peptide Trichogin GA IV in organic molecular glasses were considered in detail in reviews.[8,10,14] No aggregation was observed in polar media, whereas in glasses of low polarity the number of molecules in aggregates (N) varied from 3.1 to 4.3 depending on the type of the system. For spin-labelled Trichogin dimers (two molecules covalently bound in 'head-to-tail' fashion) in a chloroform–toluene mixture, the number N varies from 2 to 3 and the interspin distance varies from 3.0 to 4.5 nm.[79] As the concentration increases, the formation of tetramers occurs.[80]

A PELDOR study of aggregation of spin-labelled zervamycin IIA (fungal hexadecapeptide) in a glassy toluene–methanol mixture at 77 K revealed the presence of aggregates with antiparallel orientation of the peptide molecules.[81]

Aggregation of spin-labelled peptide alamethicin in polar and non-polar molecular glasses was studied.[82] The peptide molecule contains 20 amino acid residues.

Act-Aib-Pro-Aib-Ala-Aib-Ala-Glu-Aib-Val-Aib-Gly-

-Leu-Aib-Pro-Val-Aib-Glu-Gln-Phol.

The compound possesses the properties of an antibiotic. Samples spin-labelled at position 16 by replacing the amino-isobutyric acid residue by the TOAC spin label were studied. No aggregation was observed in the polar glass, in contrast to the glass of low polarity (chloroform–toluene mixture). It was found that the number of molecules in the aggregate is rather large and varies from 6 to 8.

Aggregation of spin-labelled peptides Trichogin GA IV in biological membranes was studied.[68,69] At a concentration of 2.2 mol.%, the peptide is uniformly distributed in egg L-α-phosphatidylcholine membrane.[68] The addition of cholesterol (up to 16.5 mol.%) led to an increase in the local peptide concentration. No peptide aggregation occurred at low peptide concentration in model phospholipid membranes (peptide : lipid ratio lower than 1 : 100).[69] An increase in the peptide concentration in the model phospholipid membranes to a peptide : lipid ratio of 1 : 20 caused the formation of dimeric aggregates with an average interspin distance of nearly 2.5 nm.

Peptide aggregation with an increase in the peptide concentration seems to be of fundamental importance for the appearance of membrane channels. A unique advantage of the PELDOR technique consists in the possibility of determining the number and characteristic size of molecules in aggregates.

3. Nanostructure of ionomers

Ionomers are polymers bearing ionic end groups.[83,84] The ionomer structure comprises ionic clusters a few nanometres in size. The intercluster distance is of the same order of magnitude. These parameters of the nanostructure of ionomers based on a polyisoprene/polystyrene copolymer were estimated in a PELDOR study using ionic spin probes.[85–87] The surface of ion clusters is accessible to such probes. The characteristic interparticle distance in the cluster was about

2 nm and the characteristic cluster – cluster distance was nearly 5 nm. The results obtained were considered in more detail in reviews.[10, 13]

4. Detection of structural transformations in materials

The mechanism of formation of mesoporous materials (MCM-41 and SBA-15) from the starting micellar compounds in the presence of spin probes was studied by the method of ESEEM through electron – nuclear interactions.[88–91] In different stages of the reaction the sample was cooled to 77 K and the ESEEM through the interaction of the spin-probe unpaired electron with deuterium present in the starting compounds was recorded. A number of stages of the formation of the materials were observed and interpreted.

5. Profile of water penetration into biomembranes

The depth of water penetration into a biomembrane is an important characteristic that governs transport of polar and charged particles across membranes and the energy characteristics of protein embedding in them.[92–95] The content of water in the local environment of the spin label was measured using the ESEEM effect due to hyperfine interaction of the spin-label unpaired electron with deuterium nuclei in the molecules of heavy water used for hydration of membranes.[96–99] The use of heavy water is due to the fact that, first, the amplitude of deuterium modulation much exceeds that of proton modulation. Second, this allows the contribution of the protons of biomolecules to the ESEEM effect to be separated. Using the SDSL technique, one can determine the local concentration of water in the nearest environment of the spin label by the ESEEM method. The estimated spatial resolution of the method was about 0.5 nm.

Studies were carried out using either lipids spin-labelled at different positions of the aliphatic chain in DL-α-dipalmitoyl phosphatidylcholine (DPPC) model phospholipid membranes[96, 99] or spin probes based on *p*-doxylstearic acid (n = 5, 7, 12, 16) in multilayered egg phosphatidylcholine liposomes.[97, 98] The experimental techniques employed were two-pulse echo[96–98] and stimulated echo,[99] the latter being much more accurate.

The experimental temporal oscillations of stimulated ESEEM signals and the corresponding cosine-Fourier-transformed spectra are similar to those shown in Fig. 3. The spectrum exhibits a narrow line and a broad background component (see Fig. 3 *b*). According to theoretical analysis,[99] the narrow line is due to the interaction with free water, whereas the broad component arises from the interaction with bound water that forms a complex with the nitroxide radical. For samples labelled at different positions of the lipid chain, the amplitudes (spectral density) of the deuterium line are appreciably different. In Fig. 5 this amplitude is plotted *vs.* label position (amplitudes of the narrow line and broad component appeared to be in proportion to each other). As the label 'moves' into membrane's interior, the amplitude (and, hence, water concentration) decreases. In the presence of cholesterol, the concentration of water near the membrane surface is higher and decreases much more abruptly on 'moving' into the membrane interior. The drop occurs near the C(8) atom in the lipid chain. The smooth decrease in the absence of cholesterol can be explained by 'entanglement' of lipid chains (cholesterol favours ordering of lipid molecules).

The results mentioned above were also considered in a review.[100]

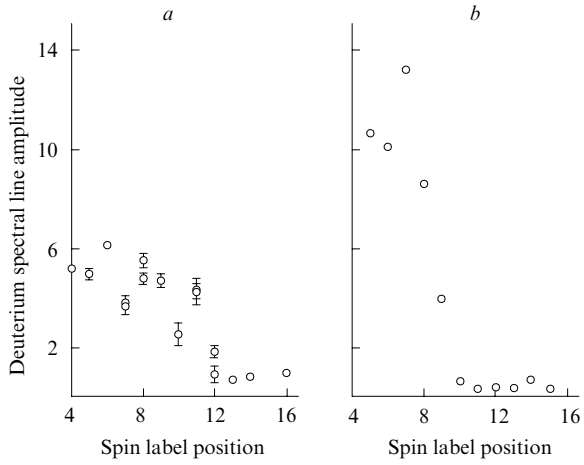


Figure 5. Spectral line amplitudes at 2.2 MHz (see Fig. 3) plotted *vs.* label position in the lipid chain in model phospholipid membranes hydrated with deuterium water.
Cholesterol-free DPPC membrane (*a*) and cholesterol-containing DPPC membrane (*b*).

6. Localisation of peptides and other biomolecules in membranes

A series of spin probes, namely, *p*-doxylstearic acid (n = 5, 7, 10, 12, 16) in DPPC and dihexadecyl prosphate (DHP) vesicles were studied by the ESEEM method.[101] The ESEEM effect was induced by the interaction between the unpaired electron in the doxyl group and ^{31}P nuclei of the polar heads of the lipid vesicles. Based on the results obtained, one can draw conclusions about localisation of the spin probe relative to the membrane surface. It was found that the spin probe penetrates about 0.5 nm into the DHP vesicles.

At present, considerable attention is given to studies of the supramolecular structure of membrane – peptide systems. A 'classical' object of such studies is peptide Trichogin GA IV. The peptide helix is 1.6 nm long, which is about half the membrane thickness. Most studies were carried out using fluorescent labels.[102–104] However, this technique has a significant drawback, namely, the labels are too bulky and can be displaced towards the membrane surface along with the peptide.[103] Therefore, it is interesting to perform corresponding spin label studies because spin labels are much more compact.

The localisation and orientation of peptide Trichogin GA IV in a phospholipid membrane were studied[67] using the effect of polarity on the parameters of HFI in c.w. EPR spectra. However, molecular motions also contribute to these interactions, thus introducing errors in experimental data. The methods based on ESEEM are free from this drawback.

The ESEEM profile of water concentration in a model phospholipid membrane[99] was used for the determination of localisation of spin-labelled peptide Trichogin GA IV in this membrane.[105] Three peptide analogues spin-labelled at different positions (1, 4 and 8) were studied.

Fmoc-TOAC-Gly-Leu-Aib^4-Gly-Gly-Leu-

-Aib^8-Gly-Ile-Leu-OMe,

Fmoc-Aib^1-Gly-Leu-TOAC-Gly-Gly-Leu-

-Aib^8-Gly-Ile-Leu-OMe,

Fmoc-Aib^1-Gly-Leu-Aib^4-Gly-Gly-Leu-

-TOAC-Gly-Ile-Leu-OMe.

Figure 6 presents the ESEEM spectra of the three samples. The peak amplitudes obtained should be compared with the amplitudes obtained for the spin labels in lipids measured

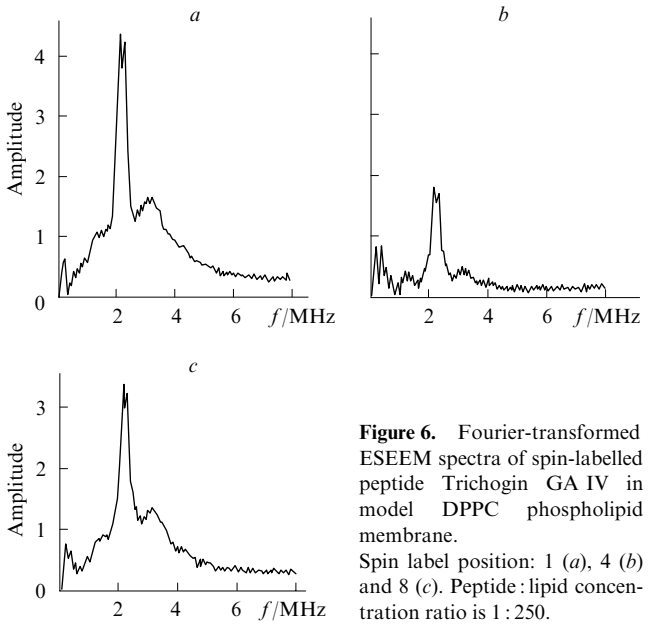


Figure 6. Fourier-transformed ESEEM spectra of spin-labelled peptide Trichogin GA IV in model DPPC phospholipid membrane.
Spin label position: 1 (*a*), 4 (*b*) and 8 (*c*). Peptide : lipid concentration ratio is 1 : 250.

under identical conditions (see Fig. 5, data in the absence of cholesterol). A comparison shows that the amplitudes for positions 1 and 8 (4.2 and 3.3 arbitrary units, see Fig. 6) are similar to those for the spin label positions in the lipids that are closer to the membrane surface than position 10 with respect to the polar head, *i.e.*, positions 1 and 8 of the spin labels in the peptide molecule are closer to the membrane surface than the spin label in position 10 in the lipid. At the same time, a comparison of the two types of data showed that position 4 in the peptide molecule is similar to position 10 in the lipid molecule. This suggests that the peptide molecule is oriented parallel to the membrane surface.

This situation is observed at small peptide : lipid concentration ratios (lower than 1 : 100). As this ratio increases to 1 : 20, the sutiation changes significantly (Fig. 7), namely, the peak amplitude for the spin-labelled position 1 appreciably decreases. Thus, as the peptide concentration increases, the peptide *N*-terminus moves deeper into the membrane interior and now the orientation of the whole molecule is similar to transmembrane one. As mentioned above, this is accompanied by peptide aggregation into dimers with a broad interspin distance distribution.

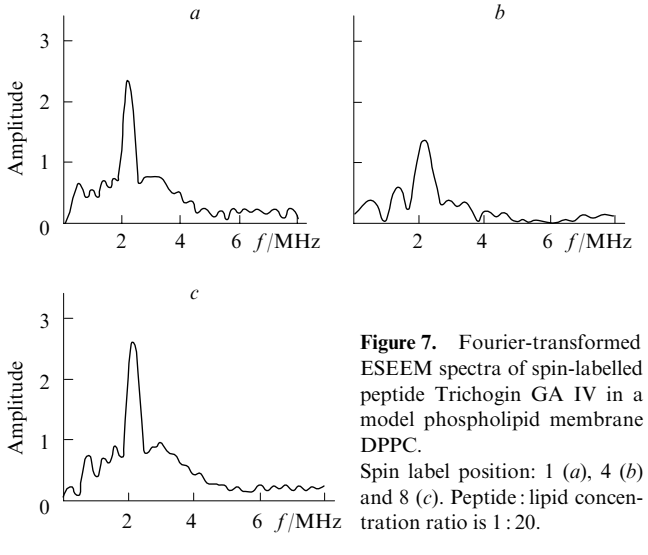


Figure 7. Fourier-transformed ESEEM spectra of spin-labelled peptide Trichogin GA IV in a model phospholipid membrane DPPC.
Spin label position: 1 (*a*), 4 (*b*) and 8 (*c*). Peptide : lipid concentration ratio is 1 : 20.

Probably, it is these changes in the supramolecular structure of a membrane with embedded peptides that are responsible for the membrane permeability. Probably, the formation of the transmembrane dimer can lead to formation of a channel in the membrane.

A similar approach was employed in a study [106] of localisation of two peptides antibiotics, a natural peptide melittin (26-mer) and a synthetic peptide (15-mer) using model membranes. The spin label was attached to the *N*-termini of the peptides (here, peptides were labelled only in one position [105]). Either D_2O-hydrated membranes or H_2O-hydrated membranes containing deuterium-substituted lipids were used. A comparison of the deuterium ESEEM peaks with the peaks of the lipids spin-labelled at different positions showed that the peptide *N*-terminus is on the membrane surface. An increase in the concentration of non-labelled peptides caused a noticeable water penetration into the membrane, which was detected from the increase in the deuterium peaks for the labelled lipids. This suggests that membrane permeability is governed by the peptide concentration.

7. Structural studies of spin-labelled photosynthetic reaction centres

The SDSL and pulsed EPR studies of the supramolecular structure of photosynthetic reaction centres of plants and bacteria began quite recently. In a PELDOR study,[107] the MTSL spin label was attached to a cysteine residue at position 156 of protein *H* in the reaction centre of the bacteria *Rhodobacter sphaeroides* R26. The distance between the spin label and the primary quinone electron acceptor Q_A was found to be 3.05 ± 0.05 nm. The results of measurements were compared with the results of molecular dynamics calculations. It was concluded that the accuracy of measurements is sufficient for detection of structural changes that can be expected upon transfer of an electron.

V. Studies of the dynamics of spin-labelled systems

1. Rotation of methyl groups in nitroxide radicals

The paramagnetic fragment NO in the nitroxide radicals is most often shielded by four methyl groups. Generally, rotation of methyl groups has little effect on the EPR spectral shape; however, in some cases this influence can be significant. Therefore, proper use of EPR spectroscopy in the method of spin labels and probes requires information on the parameters of this motion. Studies of nitroxide radicals aimed at determining the rotational correlation times and the amplitudes of accompanying HFC fluctuations in a wide temperature range have been reported only very recently. They were carried out by the ESEEM method (see above); here the ESEEM effect is due to spontaneous changes in the magnetic parameters of radicals induced by the three-pulse stimulated ESE sequence.[42–44]

The Fourier transformed stimulated ESE spectra of some nitroxide radicals in glassy toluene, ethanol and water – glycerol (1 : 1) mixture at 77 and 90 K revealed [42] the appearance of intense peaks in a broad frequency range from 0 to 15 MHz. The peak at 15 MHz, which is due to the interaction with the matrix protons, showed no temperature dependence, whereas the peaks at lower frequencies became much more intense with an increase in T. The effect was attributed to rotation of methyl groups. The Fremy salt nitroxide radical contains no methyl groups; a reference experiment with this compound showed no effect.

A study [43] of nitroxide radicals in *o*-terphenyl and glycerol in the temperature range 120 – 260 K also revealed intense peaks that became more intense with increasing T. This effect was attributed to relaxation of methyl protons. The nuclear

relaxation rate was determined from the kinetics of peak growth. The rotational correlation time of methyl groups was determined from the relaxation rate using the Redfield theory.[20] The Arrhenius parameters of this rotation are as follows: the energy barrier lies in the range 1300 – 1500 K and the pre-exponent is about 10^{12} s^{-1}.

2. Fast small-amplitude orientation mobility of spin probes in molecular glasses

Spectral transformations with an increase in τ (see Fig. 4) correspond to the model of small-amplitude stochastic librations. In this case, the relaxation anisotropy is determined using expression (4). The results of these calculations and the experimental data are in excellent agreement.[22] The whole set of the spectra recorded at different τ was calculated using only one fitting parameter, namely, the product $\langle\alpha^2\rangle\tau_c$, which is proportional to the relaxation rate $\langle\Delta\omega^2\rangle\tau_c$.

The c.w. EPR spectra are also consistent with the model of fast small-amplitude motions.[108] Note that c.w. EPR experiments with glassy liquids and other disordered systems are often treated in terms of such motion models as continuous Brownian diffusion in the angular space or discrete rotation by an arbitrary or fixed angle (accounting or ignoring the motion anisotropy).[109] These models assume an infinite molecular motion in the angular space. However, there are data that contradict the infinite character of motion. For instance, if polarised light 'burns out' a particular orientation of photosensitive molecules, one can monitor how the spectral 'hole' broadens with time.[110] These experiments permit immediate measurements of the rate of the infinite angular motion. It was found that the rate determined is many orders of magnitude lower than the rate determined by analysing the EPR spectra of spin probes of similar size. Therefore, the models of infinite motions are inappropriate for the description of the motion in highly viscous media and molecular glasses, often despite good agreement between theory and experiment.[109]

The behaviour of the echo-detected EPR spectra with an increase in τ (see Fig. 4) is typical of spin labels and spin probes in disordered media including biosystems. Moreover, it is also characteristic of other types of paramagnetic species that exhibit anisotropic EPR spectra, namely, metal complexes,[111] semiquinone radicals in high-field EPR[112] and molecules in triplet excited states.[113] Thus, it becomes clear that here we deal with some universal basic regularities of the molecular dynamics in such systems. Unusual character of the molecular dynamics in disordered media has long been reported in studies carried out by various physical methods, namely, light scattering,[114] single-molecule spectroscopy,[115] dielectric relaxation,[116] neutron scattering,[117] Mössbauer absorption,[118] *etc*. Despite numerous experimental data, the nature of the phenomena is still to be clarified.

Interesting information on the properties of this motion can be obtained using echo-detected EPR spectroscopy. Observation of anisotropic relaxation in echo-detected EPR spectroscopy indicates that orientational motion of the whole molecule occurs in the system. A study of the dynamics of spin probes of different structure and in different glassy solvents[119] allowed one to establish with certainty that the motion depends on the nature of the solvent rather than the type of the spin probe. Probes used in these studies were 0.3 to 5 nm in size; therefore, it is clear that it is co-operative molecular dynamics, *i.e*., the motion occurs by collective rearrangements in the molecular structure, being supramolecular in character. The size of the molecular cluster is a few nanometres. In the case of simple low-molecular-mass glasses the motion is also supramolecular in character.

The principal value of the HFC tensor $\langle A_{ZZ}\rangle$ averaged by fast motions can be determined with ease from c.w. EPR spectra (see Fig. 1). Typical results obtained for molecular glasses are shown in Fig. 8 *a*. The temperature dependence of $\langle A_{ZZ}\rangle$ is linear at low temperatures and becomes much steeper above a certain temperature. Using these data and relation (5), it is possible to obtain the temperature dependence of $\langle\alpha^2\rangle$ (Fig. 8 *b*).

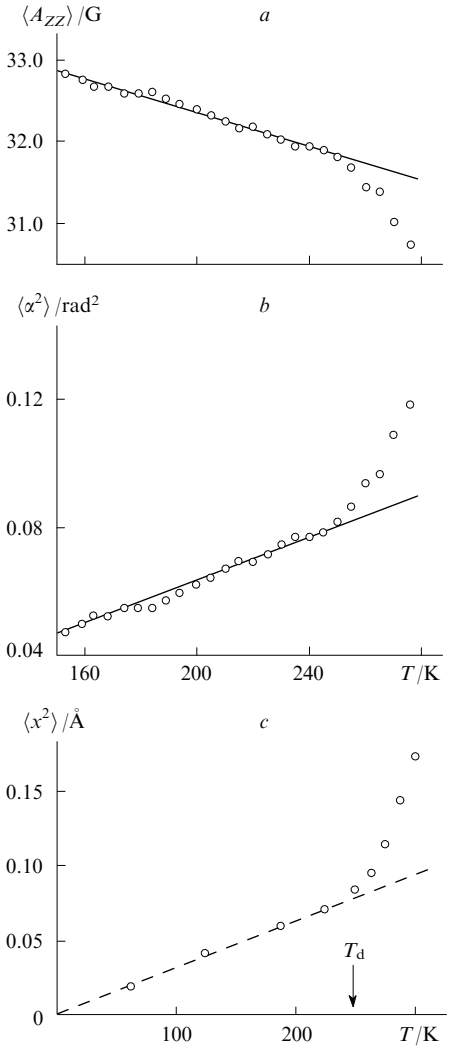


Figure 8. Typical temperature dependences of the spectral splitting $\langle A_{ZZ}\rangle$ (see Fig. 1) obtained for nitroxide spin probes in *o*-terphenyl (*a*), root-mean-square angles of deviation from equilibrium position obtained from relationship (5) (*b*) and root-mean-square fluctuations of atomic positions relative to the equilibrium position $\langle x^2\rangle$ obtained from neutron scattering studies (*c*).
T_d is dynamic transition temperature.

3. Dynamic low-temperature transition in disordered media

Neutron scattering[117, 120] and Mössbauer absorption[118] studies of atomic vibrations in molecular disordered (including biological) media (in the latter case the substance under study contains ^{57}Fe ions) revealed a clearly defined transition from harmonic to anharmonic motion on raising the temperature. The effect manifests itself as transition from the linear temperature dependence of the root-mean-square atomic displacement $\langle x^2\rangle$ (this is characteristic of harmonic motion) to a steeper dependence with an increase in temperature. The transition is only characteristic of the disordered media. A feature of the crystalline state is a linear temperature dependence in the whole temperature range. This transition is

called the dynamic transition; the transition temperature is denoted by T_d (Fig. 8 *c*).

Biosystems have the T_d temperatures lying in the range 200 – 230 K.[120] The physiological activity of biosystems manifests itself only above T_d. At present, the nature of this transition and its importance for biosystems have been subjects of intensive studies. Interestingly, these T_d values are similar to the minimum air temperatures on the Earth.

Valuable information on the molecular dynamics can be obtained by echo-detected EPR spectroscopy of spin labels and spin probes. Noteworthy is an analogy between the EPR data and the neutron scattering data shown in Figs 8 *b* and 8 *c*, respectively. Neutron scattering is sensitive to motions at frequencies higher than 10^9 s^{-1} (Mössbauer absorption is sensitive to motions at frequencies higher than 10^7 s^{-1}). These frequencies are of the same order of magnitude as that required for librational narrowing of EPR spectra (10^8 s^{-1}). The characteristic motion amplitudes $\langle x^2 \rangle$ (see Refs 117, 118 and 120) are also similar in magnitude to the $\langle \alpha^2 \rangle$ values shown in Fig. 8 *b* (numerical values of $\langle \alpha^2 \rangle$ expressed in squared radians and of $\langle x^2 \rangle$ expressed in squared Ångströms can be compared with allowance for the fact that the characteristic size of the molecule is $\sim$1 Å). These quantitative relations suggest that different methods deal with the same type of motion.

The applicability of c.w. EPR for measuring $\langle \alpha^2 \rangle$ is limited to non-polar media. In polar media, the measured A_{ZZ} value is additionally affected by the change in the matrix polarity, which may introduce rather large errors. In the case of echo-detected EPR, information on the motion is extracted from the rate of anisotropic relaxation, which is not affected by the polarity of the matrix.

A typical temperature dependence of the characteristic changes in the echo-detected EPR spectra in molecular glasses is shown in Fig. 9. These changes can be characterised by the relative intensity at the centre of the high-field component. At low temperatures, no changes occur, but raising the temperature causes a marked decrease in the intensity, which may be assigned to the dynamic transition.

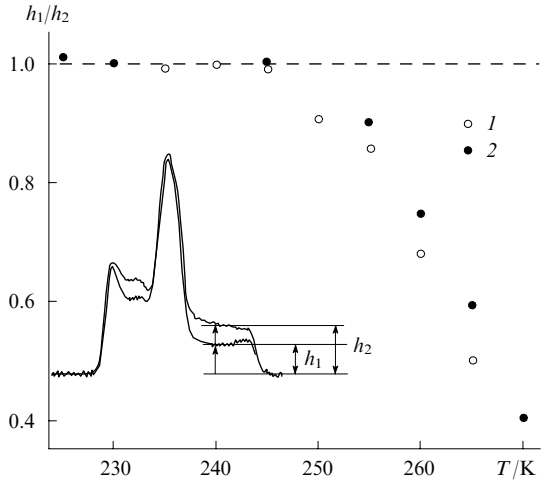


Figure 9. Typical temperature dependences of characteristic changes in echo-detected EPR spectrum induced by unfreezing of stochastic librations (nitroxide spin probe in *o*-terphenyl);
h_1/h_2 is the height ratio of the EPR spectra recorded at different temperatures and normalised to maximum amplitudes; h_2 corresponds to a temperature of 230 K (no spectral changes occur at lower temperatures). The open (*1*) and solid (*2*) circles denote data obtained for different nitroxide radicals.

The T_d values determined for molecular glasses (glycerol and *o*-terphenyl) are 195 and 245 K, respectively.[121, 122] It was found that these temperatures coincide with the T_d values determined for these glasses from neutron scattering data.[117, 123]

Thus, echo-detected EPR is a sensitive tool for determination of the temperature of the dynamic transition from harmonic to anharmonic (or stochastic) motion. Other important advantages of this technique are the relative, compared to neutron scattering and Mössbauer abrosption, accessibility of measurements and the possibility of SDSL studies of different fragments in complex supramolecular systems.

A rather steep decrease in the temperature dependence shown in Fig. 9 prompt that the potential of this motion seems to be temperature dependent and changes its shape above a certain temperature. Different versions are possible, namely, the potential can be essentially anharmonic or it may become a stochastic function of time.

Since the potential is determined by the structure of matter, we can say that the so-called mean order in this structure (correlations in the arrangement of atoms and molecules on the nanometre scale) changes above T_d.

4. Dynamic low-temperature transition in spin-labelled model biomembranes

Echo-detected EPR spectroscopy studies of the dynamics of DPPC lipids spin-labelled at different positions of the lipid chain in model phospholipid membranes with high content of cholesterol (50 mol.%) revealed [124] a dynamic transition, common to all positions, with T_d lying in the range 200 – 230 K. This is in agreement with the results obtained in a neutron scattering study.[93] A new phenomenon was disclosed in comparing the data for different positions in the spin label, namely, in the membrane interior the dynamic transition spans a wide temperature range and begins at 100 – 120 K.

A dynamics study of cholestane spin probe (this compound is structurally similar to cholesterol, an important membrane component)[125] also showed low-temperature motions in the membrane interior.

Different-type dynamics at different distances from the membrane surface and low-temperature motions may appear to be important for understanding the mechanisms of membrane functioning. These data may also be of interest for the development of fundamental concepts of possible mechanisms of biological tissue cryoconservation.

5. Dynamic low-temperature transition in spin-labelled complex biosystems and its interrelation with functional activity

Seed and pollen cells are interesting subjects for studies using the method of spin labels and probes. They show a remarkable ability to be stored for years without loss of vital activity. A possible explanation for this ability involves intracell glass formation. An echo-detected EPR study of spin probes introduced into the seed and pollen cells revealed a marked anisotropic relaxation at $T > 200$ K, which itself indicates glass formation.[126] These effects depend strongly on the water content in the samples. These studies are important for understanding the processes that govern the storage period of seeds and other biological objects.

Echo-detected EPR was also used to study SDSL reaction centres isolated from the photosynthetic centre of purple bacteria.[127] These objects are often used in studies of fundamental processes in photosynthesis. Cysteine residues in these centres were labelled with the MTSL spin label. A clearly defined dynamic transition was detected near 200 K. At this temperature, transfer of a photo-induced electron along the electron acceptor chain is blocked,[128 – 130] namely, electron back transfer occurs followed by recombination with the

'hole' (radical cation of bacteriochlorophyll dimer) instead of direct electron transfer from the primary quinone acceptor to the secondary one. The nature of the reversal of electron transfer direction is still to be clarified. Moreover, no correlations between this effect and the properties of complex supramolecular structure of the reaction centre were reported so far. The results of echo-detected EPR studies indicate the correlation of this effect with the dynamic transition near 200 K in the system.

6. Dynamic structure of vesicular membranes

The motion of cholestane spin probes in multilayered phospholipid vesicles in the presence of cholesterol was studied by the 2D PELDOR method.[49] At present, it is accepted that a liquid ordered phase appears in cholesterol-containing membranes in addition to conventional liquid-crystalline phase (which also exists in the absence of cholesterol). The ordered domains are called rafts. The two phases are in equilibrium; their investigations are of considerable interest from the standpoint of research on the membrane operation mechanisms. Visual studies of 2D spectra did allow one to distinguish two phases differing in the rotational diffusion rate and degree of molecular ordering (these parameters were higher in the ordered domains).

VI. Conclusion

The use of pulsed EPR in the method of spin labels and probes have been started quite recently. Spectroscopic methods appeared to be useful in conformational and aggregation studies of large biomolecules, nanostructure of matter, supramolecular structure of multicomponent systems and co-operative orientational dynamics of molecules. In some cases they show a record resolution compared to other physicochemical methods of investigation. For instance, the PELDOR technique is highly sensitive to distance measurements in the nanometre range and provides a 0.1-nm accuracy of measurements at distances of about 3 nm. Echo-detected EPR spectroscopy is a sensitive tool of investigation of small-amplitude stochastic orientational motions (down to amplitudes of $0.1-1^{\circ}$). Using this method, the temperature of dynamic transition from harmonic to anharmonic (or stochastic) motion in disordered molecular media and biosystems can be determined with ease. More and more data reported in the literature indicate that this transition is a crucially important characteristic of living systems.

Pulsed EPR techniques are continuously developed and improved. It is of great importance that the vast majority of the results discussed above were (or could be) obtained using commercially available spectrometers.

The review has been written with the financial support from the Russian Foundation for Basic Research and NWO (Joint Project No. 06-03-89 400-HBO_a), the U.S. Civilian Research and Development Foundation (Grant RUC1-2635-NO-05) and the Siberian Branch of the Russian Academy of Sciences (Integration Project No. 51).

References

1. *Spin Labeling. Theory and Application* (Ed. L J Berliner) (New York: Academic Press, 1976)
2. *Spin Labeling. Theory and Applications, Biological Magnetic Resonance* Vol. 8 (Ed. L J Berliner) (New York: Plenum, 1989)
3. *Spin Labeling. The Next Millennium, Biological Magnetic Resonance* Vol. 14 (Ed. L J Berliner) (New York: Plenum, 1998)
4. A L Buchachenko, A M Vasserman *Stabil'nye Radikaly* (Stable Radicals) (Moscow: Khimiya, 1973)
5. L B Volodarskii, I A Grigor'ev, S A Dikanov *Imidazolinovye Nitroksil'nye Radikaly* (Imidazoline Nitroxide Radicals) (Novosibirsk: Nauka, 1988)
6. K M Salikhov, A G Semenov, Yu D Tsvetkov *Elektronnoe Spinovoe Ekho i Ego Primenenie* (Electron Spin Echo and Its Applications) (Novosibirsk: Nauka, 1976)
7. A Schweiger, G Jeschke *Principles of Pulsed Electron Paramagnetic Resonance* (Oxford: Oxford University Press, 2001)
8. A D Milov, A G Maryasov, Yu D Tsvetkov *Appl. Magn. Reson.* **15** 107 (1998)
9. *Distance Measurements in Biological Systems by EPR Biological Magnetic Resonance* Vol. 19 (Eds G R Eaton, S S Eaton, L J Berliner) (New York: Kluwer Academic, Plenum, 2000)
10. S A Dzuba *Usp. Khim.* **74** 686 (2005) [*Russ. Chem. Rev.* **74** 619 (2005)]
11. T Prisner, M Rohrer, F MacMillan *Annu. Rev. Phys. Chem.* **52** 279 (2001)
12. J H Freed *Annu. Rev. Phys. Chem.* **51** 655 (2000)
13. G Jeschke *ChemPhysChem* **3** 927 (2002)
14. Yu D Tsvetkov *EPR Instrumental Methods, Biological Magnetic Resonance* Vol. 21 (Eds C L Bender, L J Berliner) (New York: Kluwer Academic, Plenum, 2004) p. 385
15. H J Steinhoff *Biol. Chem.* **385** 913 (2004)
16. C Altenbach, T Marti, H Khorana, W L Hubbell *Science* **248** 1088 (1990)
17. W L Hubbell, A Cross, R Langen, M A Lietzov *Curr. Opin. Struct. Biol.* **8** 649 (1998)
18. G E Fanucci, D S Cafiso *Curr. Opin. Struct. Biol.* **16** 644 (2006)
19. L J Libertini, O H Griffith *J. Chem. Phys.* **53** 1359 (1970)
20. C P Slichter *Principles of Magnetic Resonance* (Berlin: Springer, 1996)
21. S A Dzuba, Yu D Tsvetkov, A G Maryasov *Chem. Phys. Lett.* **188** 217 (1992)
22. E P Kirilina, S A Dzuba, A G Maryasov, Yu D Tsvetkov *Appl. Magn. Reson.* **21** 203 (2001)
23. A D Milov, K M Salikhov, M D Shchirov *Fiz. Tv. Tela* **23** 975 (1981) [a]
24. A D Milov, A B Ponomarev, Yu D Tsvetkov *Chem. Phys. Lett.* **110** 67 (1984)
25. L V Kulik, Yu A Grishin, S A Dzuba, I A Grigoryev, S V Klyatskaya, S F Vasilevsky, Yu D Tsvetkov *J. Magn. Reson.* **157** 61 (2002)
26. A A Dubinskii, Yu A Grishin, A N Savitsky, K Mobius *Appl. Magn. Reson.* **22** 369 (2002)
27. K Sale, L K Song, Y S Liu, E Perozo, P Fajer *J. Am. Chem. Soc.* **127** 9334 (2005)
28. M K Bowman, A G Maryasov, N Kim, V J DeRose *Appl. Magn. Reson.* **26** 23 (2004)
29. G Jeschke, G Panek, A Godt, A Bender, H Paulsen *Appl. Magn. Reson.* **26** 223 (2004)
30. G Jeschke, A Bender, H Paulsen, H Zimmermann, A Godt *J. Magn. Reson.* **169** 1 (2004)
31. A Weber, O Schiemann, B Bode, T Prisner *J. Magn. Reson.* **157** 277 (2002)
32. G Jeschke, H Zimmermann, A Godt *J. Magn. Reson.* **180** 137 (2006)
33. Ye Polyhach, A Godt, C Bauer, G Jeschke *J. Magn. Reson.* **185** 118 (2007)
34. V V Kurshev, A M Raitsimring, Yu D Tsvetkov *J. Magn. Reson.* **81** 441 (1989)
35. S Saxena, J H Freed *Chem. Phys. Lett.* **251** 102 (1996)
36. H Hara, T Tenno, M Shirakawa *J. Magn. Reson.* **184** 78 (2007)
37. Y W Chiang, P P Borbat, J H Freed *J. Magn. Reson.* **172** 279 (2005)
38. M Bonora, J Becker, S Saxena *J. Magn. Reson.* **170** 278 (2004)
39. G Jeschke, M Pannier, A Godt, H W Spiess *Chem. Phys. Lett.* **331** 243 (2000)
40. L V Kulik, S A Dzuba, I A Grigoryev, Yu D Tsvetkov *Chem. Phys. Lett.* **343** 315 (2001)
41. L V Kulik, S V Paschenko, S A Dzuba *J. Magn. Reson.* **159** 237 (2002)
42. L V Kulik, I A Grigor'ev, E S Salnikov, S A Dzuba, Yu D Tsvetkov *J. Phys. Chem. A* **107** 3692 (2003)

43. L V Kulik, E S Salnikov, S A Dzuba *Appl. Magn. Reson.* **28** 1 (2005)
44. L V Kulik, S A Dzuba *Zh. Srukt. Khim.* **45** 313 (2004) [b]
45. M M Hertel, V P Denysenkov, V Bennati, T F Prisner *Magn. Reson. Chem.* **43** 248 (2005)
46. E P Kirilina, T F Prisner, M Bennati, B Endeward, S A Dzuba, M R Fuchs, K Möbius, A Schnegg *Magn. Reson. Chem.* **43** S119 (2005)
47. S A Dzuba, E P Kirilina, E S Salnikov, L V Kulik *J. Chem. Phys.* **122** 094702 (2005)
48. P P Borbat, A J Costa-Filho, K A Earle, J Moscicki, J H Freed *Science* **291** 266 (2001)
49. A J Costa-Filho, Y Shimoyama, J H Freed *Biophys. J.* **84** 2619 (2003)
50. P P Zanker, G Jeschke, D Goldfarb *J. Chem. Phys.* **122** 024515 (2005)
51. T I Smirnova, A I Smirnov, S V Paschenko, O G Poluektov *J. Am. Chem. Soc.* **129** 3476 (2007)
52. R W Quine, S S Eaton, G R Eaton *Rev. Sci. Instrum.* **63** 4252 (1992)
53. M Huber, M Lindgren, P Hammarstrom, L G Martensson, U Carlsson , G R Eaton, S S Eaton *Biophys. Chem.* **94** 245 (2001)
54. C S Klug, S S Eaton, G R Eaton, J B Feix *Biochemistry* **37** 9016 (1998)
55. J S Hyde, J J Yin, W K Subczynski, T G Camenisch, J J Ratke, W Froncisz *J. Phys. Chem. B* **108** 9524 (2004)
56. W K Subczynski, A Wisniewska, J S Hyde, A Kusumi *Biophys. J.* **92** 1573 (2007)
57. F Formaggio, E Sartori, A Toffoletti, C Corvaja, L Moroder, C Toniolo *Adv. Exp. Med. Biol.* **527** 731 (2003)
58. K M Salikhov, S G Zech, D Stehlik *Mol. Phys.* **100** 1311 (2002)
59. G Jeschke, A Koch, U Jonas, A Godt *J. Magn. Reson.* **155** 72 (2002)
60. V Pfannebecker, H Klos, M Hubrich, T Volmer, A Heuer, U Wiesner, H W Spiess *J. Phys. Chem.* **100** 13428 (1996)
61. E Narr, A Godt, G Jeschke *Angew. Chem., Int. Ed.* **41** 3907 (2002)
62. J C McNulty, G L Millhauser *Distance Measurements in Biological Systems by EPR Biological Magnetic Resonance* Vol. 19 (Eds G R Eaton, S S Eaton, L J Berliner) (New York: Kluwer Academic, Plenum, 2000) p. 277
63. A D Milov, A G Maryasov, Yu D Tsvetkov, J Raap *Chem. Phys. Lett.* **303** 135 (1999)
64. A D Milov, A G Mar'yasov, R I Samoilova, Yu D Tsvetkov, J Raap, V Monaco, F Formagghio, M Crisma, C Toniolo *Dokl. Akad. Nauk* **370** 265 (2000) [c]
65. A D Milov, Yu D Tsvetkov, F Formaggio, M Crisma, C Toniolo, J Raap *J. Am. Chem. Soc.* **123** 3784 (2001)
66. M Crisma, V Monako, F Formaggio, C Toniolo, C George, J-L Flippen-Anderson *Lett. Pept. Sci.* **4** 213 (1997)
67. V Monaco, F Formaggio, M Crisma, C Toniolo, P Hanson, G L Millhauser *Biopolymers* **50** 239 (1999)
68. A D Milov, R I Samoilova, Y D Tsvetkov, F Formaggio, C Toniolo, J Raap *Appl. Magn. Reson.* **29** 703 (2005)
69. A D Milov, D A Erilov, E S Salnikov, Y D Tsvetkov, F Formaqqio, C Toniolo, J Raap *Phys. Chem. Chem. Phys.* **7** 1794 (2005)
70. O Schiemann, A Weber, T E Edwards, T Prisner, S T Sigurdsson *J. Am. Chem. Soc.* **125** 3434 (2003)
71. N Piton, O Schiemann, Y G Mu, G Stock, T Prisner, J W Engels *Nucleosides, Nucleotides and Nucleic Acids* **24** 771 (2005)
72. O Schiemann, N Piton, Y G Mu, G Stock, J W Engeels, T F Prisner *J. Am. Chem. Soc.* **126** 5722 (2004)
73. Q Xu, J F Ellena, M Kim, D S Cafiso *Biochemistry* **45** 10847 (2006)
74. D Hilger, H Jung, E Padan, C Wegener, K P Vogel, H J Steinhoff, G Jeschke *Biophys. J.* **89** 1328 (2005)
75. G Jeschke, A Godt *ChemPhysChem* **4** 1328 (2003)
76. S Steigmiller, M Borsch, P Graber, M Huber *Biochim. Biophys. Acta, Bioenergetics* **1708** 143 (2005)
77. A T Fafarman, P P Borbat, J H Freed, R Kirshenbaum *Chem. Commun.* 377 (2007)
78. Q Cai, A K Kuznetzov, W L Hubbell, I S Haworth, G P C Gacho, N Van Eps, K Hideg, E J Chambers, P Z Qin *Nucleic Acids Res.* **34** 4722 (2006)
79. A D Milov, Yu D Tsvetkov, F Formaggio, S Oancea, C Toniolo, J Raap *J. Phys. Chem. B* **107** 13719 (2003)
80. A D Milov, Yu D Tsvetkov, F Formaggio, M Crisma, C Toniolo, J Raap *J. Pept. Sci.* **9** 690 (2003)
81. A D Milov, Yu D Tsvetkov, E Yu Gorbunova, L G Mustaeva, T V Ovchinnikova, J Raap *Biopolymers* **64** 326 (2002)
82. A D Milov, R I Samoilova, Yu D Tsvetkov, C Peggion, F Formaggio, C T Toniolo, J Raap *Dokl. Akad. Nauk* **406** 341 (2006) [c]
83. S Schlick *Ionomers*: *Characterization Theory and Applications* (Boca Raton, FL: CRC Press, 1996)
84. A Eisenberg, J-S Kim *Introduction to Ionomers* (New York: Wiley-Interscience, 1998)
85. M Pannier, V Schadler, M Schops, U Wiesner, G Jeschke, H W Spiess *Macromolecules* **33** 7812 (2000)
86. M Pannier, M Schops, V Schadler, U Wiesner, G Jeschke, H W Spiess *Macromolecules* **34** 5555 (2001)
87. G Jeschke *Macromol. Rapid Commun.* **23** 227 (2002)
88. D Baute, V Frydman, H Zimmermann, S Kababya, D Goldfarb *J. Phys. Chem. B* **109** 7807 (2005)
89. S Ruthstein, V Frydman, D Goldfarb *J. Phys. Chem. B* **108** 9016 (2004)
90. S Ruthstein, V Frydman, S Kababya, M Landau, D Goldfarb *J. Phys. Chem. B* **107** 1739 (2003)
91. J Y Zhang, P J Carl, H Zimmermann, D Goldfarb *J. Phys. Chem. B* **106** 5382 (2002)
92. K Aman, E Lindahl, O Edholm, P Hakansson, P-O Westlund *Biophys. J.* **84** 102 (2003)
93. J Fitter, R E Lechner, N A Dencher *J. Phys. Chem. B* **103** 8036 (1999)
94. J Milhaud *Biochim. Biophys. Acta, Biomembranes* **1663** 19 (2004)
95. S Y Bhide, M L Berkowitz *J. Chem. Phys.* **123** 224702 (2005)
96. R Bartucci, R Guzzi, D Marsh, L Sportelli *Biophys. J.* **84** 1025 (2003)
97. V Noethig-Laslo, P Cevc, D Arcon, M Sentjurc *Origins Life Evol. Biosphere* **34** 237 (2004)
98. V Noethig-Laslo, P Cevc, D Arcon, M Sentjurc *Appl. Magn. Reson.* **27** 303 (2004)
99. D A Erilov, R Bartucci, R Guzzi, A A Shubin, A G Maryasov, D Marsh, S A Dzuba, L Sportelli *J. Phys. Chem. B* **109** 12003 (2005)
100. R Bartucci, D A Erilov, R Guzzi, L Sportelli, S A Dzuba, D Marsh *Chem. Phys. Lipids* **141** 142 (2006)
101. V V Kurshev, L Kevan *J. Phys. Chem.* **99** 10616 (1995)
102. R F Epand, R M Epand, V Monaco, S Stoia, F Formaggio, M Crisma, C Toniolo *Eur. J. Biochem.* **266** 1021 (1999)
103. R D Kaiser, E London *Biochim. Biophys. Acta* **1375** 13 (1998)
104. C Mazzuca, L Stella, M Venanzi, F Formaggio, C Toniolo, B Pispisa *Biophys. J.* **88** 3411 (2005)
105. E S Salnikov, D A Erilov, A D Milov, Yu D Tsvetkov, C Peggion, F Formaggio, C Toniolo, J Raap, S A Dzuba *Biophys. J.* **91** 1532 (2006)
106. R Carmieli, N Papo, H Zimmermann, A Potapov, Y Shai, D Goldfarb *Biophys. J.* **90** 492 (2006)
107. I V Borovykh, S Ceola, P Gajula, P Gast, H J Steinhoff, M Huber *J. Magn. Reson.* **180** 178 (2006)
108. S V Paschenko, Yu V Toropov, S A Dzuba, Yu D Tsvetkov, A Kh Vorobiev *J. Chem. Phys.* **110** 8150 (1999)
109. J S Hwang, R P Mason, L-P Hwang, J H Freed *J. Phys. Chem.* **79** 489 (1975)
110. A K Vorobiev, V S Gurman, T A Klimenko *Phys. Chem. Chem. Phys.* **2** 379 (2000)
111. R Husted, J L Du, S S Eaton, G R Eaton *Magn. Reson. Chem.* **33** S66 (1995)
112. A Schnegg, M Fuhs, M Rohrer, W Lubitz, T F Prisner, K Mobius *J. Phys. Chem. B* **106** 9454 (2002)
113. A Barbon, M Bortolus, M Brustolon, A Comotti, A L Maniero, U Segre, P Sozzani *J. Phys. Chem. B* **107** 3325 (2003)

114. N V Surovtsev, J A H Wiedersich, V N Novikov, E Rössler *Phys. Rev. B* **58** 14888 (1998)
115. E Barkai, A V Naumov, Yu G Vainer, M Bauer, L Kador *Phys. Rev. Lett.* **91** 075502 (2003)
116. J P Johari *Ann. N.Y. Acad. Sci.* **279** 117 (1976)
117. A Tölle, H Zimmermann, F Fujara, W Petry, W Schmidt, W Schober, J Wuttke *Eur. Phys. J., B* **16** 73 (2000)
118. F G Parak *Curr. Opin. Struct. Biol.* **13** 552 (2003)
119. E P Kirilina, I A Grigoriev, S A Dzuba *J. Chem. Phys.* **121** 12465 (2004)
120. G Galiskan, R M Briber, D Thirumalai, V Garein-Sakai, S A Woodson, A P Sokolov *J. Am. Chem. Soc.* **128** 32 (2006)
121. S A Dzuba, E P Kirilina, E S Salnikov *J. Chem. Phys.* **125** 054502 (2006)
122. S A Dzuba, E S Salnikov, L V Kulik *Appl. Magn. Reson.* **30** 637 (2006)
123. J Wuttke, W Petry, G Coddens, F Fujara *Phys. Rev. E* **52** 4026 (1995)
124. D A Erilov, R Bartucci, R Guzzi, D Marsh, S A Dzuba, L Sportelli *Biophys. J.* **87** 3873 (2004)
125. S A Dzuba, H Watari, Y Shimoyama, A G Maryasov, Y Kodera, A Kawamori *J. Magn. Reson., Ser. A* **115** 80 (1995)
126. J Buitink, S A Dzuba, F A Hoekstra, Yu D Tsvetkov *J. Magn. Reson.* **142** 364 (2000)
127. I V Borovykh, P Gast, S A Dzuba *Appl. Magn. Reson.* **31** 159 (2007)
128. Q Xu, M R Gunner *Biochemistry* **40** 3232 (2001)
129. M Bixon, J Jortner *J. Phys. Chem.* **90** 3795 (1986)
130. G Feher, M Y Okamura, D Kleinfeld *Protein Structure: Molecular and Electronic Reactivity* (Eds R Austin, E Buhks, B Chance, D De Vault, P L Dutton, H Frauenfelder, V I Goldanskii) (New York: Springer, 1987) p. 399

[a] — *Phys. Solid. State (Engl. Transl.)*
[b] — *J. Struct. Chem. (Engl. Transl.)*
[c] — *Dokl. Chem. (Engl. Transl.)*